Materials and Design 51 (2013) 513–521

Contents lists available at SciVerse ScienceDirect

Materials and Design

journal homepage: www.elsevier.com/locate/matdes

Technical Report

Application of Taguchi approach to optimize of FSSW parameters on joint properties of dissimilar AA2024-T3 and AA5754-H22 aluminum alloys

Yahya Bozkurt *, Mustafa Kemal Bilici

Marmara University, Technical Education Faculty, Department of Materials Technology, 34722 Göztepe, Istanbul, Turkey

ARTICLE INFO

Article history:
Received 27 February 2013
Accepted 19 April 2013
Available online 30 April 2013

ABSTRACT

In this study, the effect of plate positioning on mechanical properties of dissimilar lap joints was investigated by friction stir spot welding (FSSW) process. The determination of the welding parameters plays an important role for the weld strength. For the effective use of the dissimilar aluminum joints, the FSSW must have an adequate strength. The quality of the joint was evaluated by examining the characteristics of the joining efficiency as a result of the lap-shear tensile test. Four process parameters were selected: the tool rotation speed, dwell time, tool plunge depth, and tilt angle.

The process parameters were optimized by Taguchi technique based on Taguchi's L9 orthogonal array. The optimum welding process parameters were predicted, and their percentage of contribution was estimated by applying the signal-to-noise ratio and analysis of variance. The experimental results showed that the positioning of the plates played an important role on the strength of the joints. Finally, the results were confirmed by further experiments.

Crown Copyright © 2013 Published by Elsevier Ltd. All rights reserved.

1. Introduction

Weight saving in the automotive industry is becoming increasingly important and can be enhanced by using a light-weight aluminum alloy for vehicles; particularly for closure panels such as hoods, deck lids, and liftgates [1]. The demand for producing joints of dissimilar materials which can provide appropriate mechanical properties and good cost reduction is continuously increasing due to their advantages [2]. The problems arising in realizing welded joints from sheets of different materials that are difficult to obtain by employing commonly used technologies, lead to a widespread use of new techniques of welding. Resistance spot welding (RSW), currently the most commonly used joining technique in the vehicle industry, has applications for low-carbon, high-strength, and coated steels. However, RSW of aluminum alloy sheets is fraught with many disadvantages, which include porosity and cracks. Industrial interests principally focus on FSSW [1–3].

Therefore, solid-state welding is an attractive alternative for joining aluminum alloys. FSSW is a solid-state welding process, which was developed by Mazda Motor Corporation and Kawasaki Heavy Industries in 2003 to lap join aluminum sheets. Both FSW, invented by The Welding Institute (TWI) in 1991, and FSSW, a variant of FSW process, are promising joining processes for welding aluminum alloys in butt and lap positions, respectively, in the automotive industry [4–8].

FSSW is a specially designed rotating cylindrical tool with varying geometry, and a probe pin is first plunged into the upper sheet. When the rotating tool contacts the upper sheet, a downward force is applied, whereas a backing tool beneath the lower sheet supports this downward force. The downward force and the rotational speed are maintained for an appropriate time to generate frictional heat. Then, heated and softened material adjacent to the tool deforms plastically, and a solid-state bond is made between the surfaces of the upper and lower sheets. Finally, the tool is drawn out of the sheets, and the protruded pin leaves a characteristic exit hole in the middle of the joint [3].

The most significant advantage of the FSSW process compared to the conventional welding processes is that the joint can be produced without melting the base metal [9].

A schematic illustration of the FSSW process is shown in Fig. 1 [10]. The process is applied to join the two metal sheets in lap configuration. A rotating tool with a probe pin plunges into the upper sheet and a backing tool beneath the lower sheet supporting the downward force (Fig. 1a). The tool downward force, the tool rotational speed, and tool shoulder are maintained for an appropriate time to generate frictional heat. Then, the heated and softened material adjacent to the tool deforms plastically, and a solid-state bond is produced between the surfaces of the upper and lower sheets (Fig. 1b). Finally, the tool is drawn out of the sheets as shown in Fig. 1c [9,11].

* Corresponding author. Tel.: +90 216 336 57 70; fax: +90 216 337 89 87.
E-mail addresses: ybozkurt@marmara.edu.tr (Y. Bozkurt), mkbilici@marmara.edu.tr (M.K. Bilici).

0261-3069/$ - see front matter Crown Copyright © 2013 Published by Elsevier Ltd. All rights reserved.
http://dx.doi.org/10.1016/j.matdes.2013.04.074

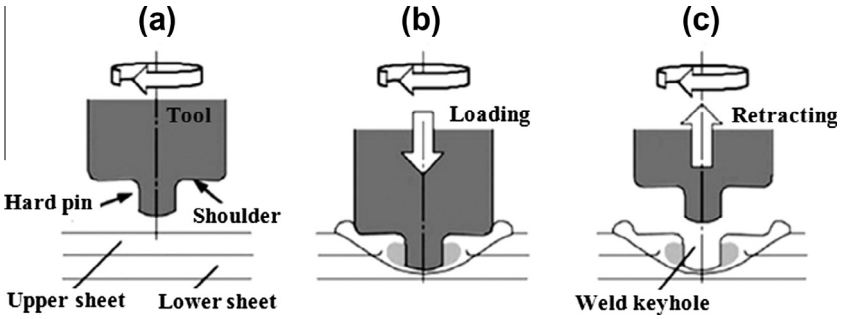


Fig. 1. A schematic illustration of the FSSWprocess: (a) plunging; (b) bonding; (c) drawing out [10].

In order to investigate the efficiency of FSSW process parameters, researchers follow the conventional experimental procedures, i.e., varying one parameter at a time while keeping the other parameters constant. This conventional parametric design of the experimental approach is time consuming and requires excessive resources. In order to solve this problem, there are different methods of achieving the desired output variables by developing new models. The Taguchi method is one of the techniques that could be applied to optimize the welding parameters. The Taguchi method has been found to be a simple and robust technique for optimizing the welding parameters [12]. Optimization of the process parameters is the key step in the Taguchi method to achieving a high quality without increasing the cost. This is because the optimization of the process parameters can improve the quality, and the optimal process parameters obtained from the Taguchi method are insensitive to the variation of the environmental conditions and other noise factors [13].

Recently, some reports have been available on the FSSW of similar and dissimilar alloys, such as joining of Al alloys [14,15], dissimilar Al alloys [16], Mg alloys [17], steels [18], Al–Mg [19], Al–steel [20], and Mg–steel [21]. But no systematic study has been reported so far to correlate the process parameters and lap-shear fracture load (LSFL) properties of FSSWed dissimilar aluminum alloys using Taguchi method as known by the authors.

Considering the above fact, the aim of this research was to analyze the effect of each processing parameter (i.e. tool rotation speed, dwell time, tool plunge depth, and tilt angle) by the Taguchi L9 method on the optimum LSFL of FSSWed dissimilar Al-alloy sheets.

2. Experimental procedure

In this study, AA2024-T3 and 5754-H22 alloy sheets (namely AA2024-T3 and 5754-H22 alloys) with the thicknesses of 1.6 and 1.5 mm, respectively, were used to produce dissimilar FSSW lap joints as shown in Fig. 2.

Trial experiments were carried out according to the principles of the design of the experiments in order to determine the effect of the main process parameters. An L9 orthogonal array with five columns and nine rows was applied. The experimental layout for the three welding parameters using the L9 orthogonal array is shown in Table 1. Since the L9 orthogonal array has five columns, each welding parameter is assigned to a column, and the last column is left empty for the error in the experimental studies. The orthogonality is not lost by letting one column of the array empty [22].

The chemical compositions and mechanical properties of these Al alloys sheets are given in Table 2. The dimensions of all spot-welded test specimens were 25×100 mm with a 25×25 mm overlap area. All the FSSW experiments were conducted with an FSW adapted universal milling machine.

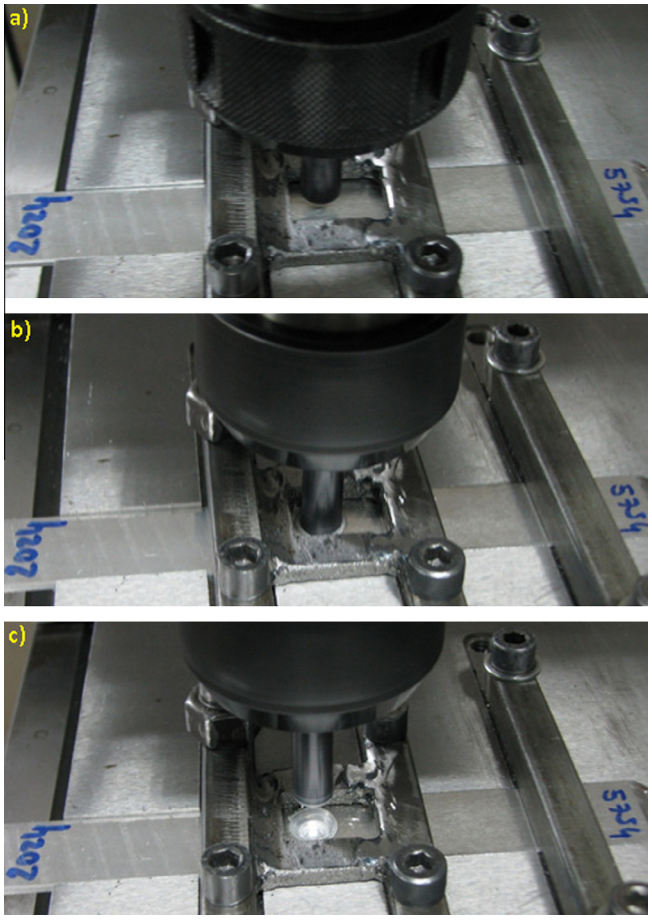


Fig. 2. Dissimilar FSSW process: (a) the rotating tool prior to the penetration into the lap joint; (b) the tool shoulder makes contact with the part, creating heat and the joint zone; (c) the retraction of the tool from the lap joint zone.

The FSSW tool was made of hot work tool steel (i.e., AISI H13) coated with Aluminum Titanium Nitride (AlTiN) and had a hardness of 56 HRC. The shoulder diameter, pin diameter, and pin length of FSSW tool were 10 mm, 4 mm, and 2.35 mm, respectively. The lap joint configuration was used to produce the FSSW joints. The rolling direction of the sheets and the joint was originally achieved by securing the sheets in position using mechanical clamps.

Two case test specimens produced regarding the position of Al sheets as shown in Table 3. In the first case, indicated as Case I in the remaining section of the article, the AA2024-T3 sheet was placed above the AA5754-H22. In the second case indicated as Case II, the positions of the sheets in Case I were reversed.

Table 1
Experimental layout using an L9 orthogonal array.

Experiment number	FSSW process parameters				Error E
	A Tool rotation speed (rpm)	B Tilt angle (°)	C Tool plunge depth (mm)	D Dwell time (s)	
1	1500	0	2.45	2	
2	1500	2	2.55	5	
3	1500	3	2.65	10	
4	2100	0	2.45	2	
5	2100	2	2.55	5	
6	2100	3	2.65	10	
7	3000	0	2.45	2	
8	3000	2	2.55	5	
9	3000	3	2.65	10	

Table 2
The chemical composition and mechanical properties of the aluminum sheets.

Alloy	Mechanical properties		Chemical composition (wt.%)								
	Tensile strength (MPa)	Elongation (%)	Al	Si	Fe	Cu	Mn	Mg	Zn	Ti	Cr
AA2024-T3	435	17	93.11	0.07	0.14	4.5	0.65	1.5	0.01	0.02	–
AA5754-H22	245	14	95.29	0.25	0.31	0.02	0.38	3.2	0.18	0.12	0.23

Table 3
Material combination of FSSWed sheets.

Upper sheet		Lower sheet		Combination
Material	Thickness (mm)	Material	Thickness (mm)	
AA2024-T3	1.6	AA5754-H22	1.5	Case I
AA5754-H22	1.5	AA2024-T3	1.6	Case II

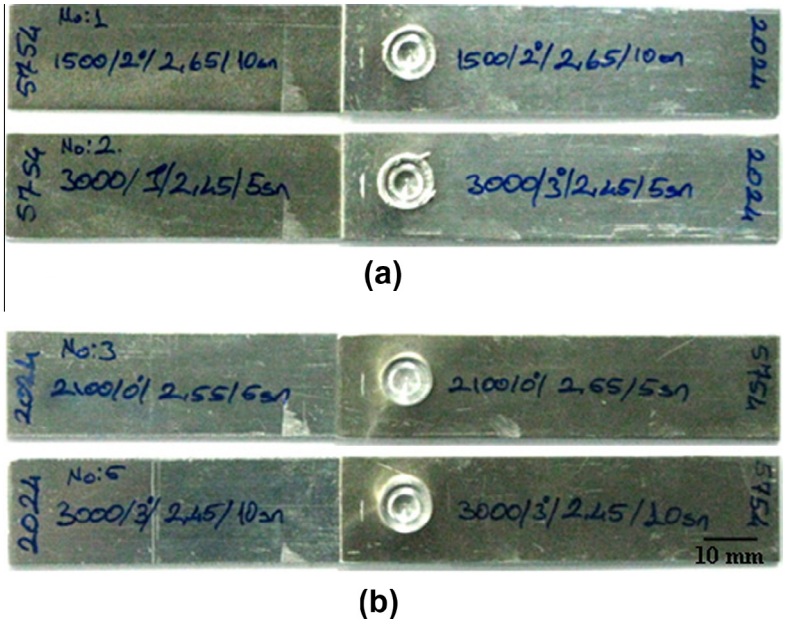


Fig. 3. Lap-shear specimens: (a) FSSW joints of Case I and (b) Case II.

It is worth mentioning that in both cases, the upper sheet was in touch with the shoulder of the welding tool during the FSSW process. Fig. 3 shows two typical lap-shear joints associated with Case I (Fig. 3a) and Case II (Fig. 3b).

For the FSSW process, the important process parameters are the tool geometry, tool rotational speed, tool tilt angle, tool plunge depth, and dwell time. The rotating tool was plunged into the workpieces with a certain plunge rate down to the required depth with an accuracy of ±0.02 mm.

The lap-shear tensile tests were carried out at room temperature, according to JIS Z3136 [23] by a universal type tensile test machine as shown in Fig. 4. Fig. 4a and b shown before the test

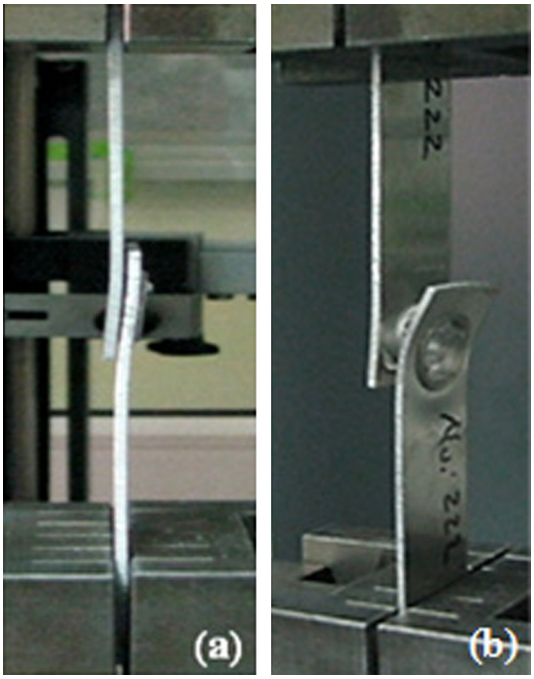


Fig. 4. Lap-shear tensile test operation of the dissimilar FSSW joints: (a) before the test and, (b) after the test.

and after the test. At least three specimens were tested under the same conditions to guarantee the reliability of the results.

3. Results and discussion

3.1. Fracture appearances of dissimilar FSSW joints

Fig. 5 illustrates the fracture surfaces of the upper and lower sheets of FSSW joints the after lap-shear tensile tests. These FSSW joints are shown in Fig. 5a, c and d which revealed that the minimum and maximum LSFL values for Case I and Case II, respectively. As seen, the upper surfaces of the joints look like a button with a central hole in both joints, as reported by [4]. The maximum LSFL value was acquired from the joint of Case I using a tool rotation speed 1500 rpm, tool tilt angle 2°, tool plunge depth of 2.65 mm, and tool dwell time of 10 s (1500/2/2.65/10 welding parameters). For Case II, maximum LSFL value was obtained using 2100/0/2.55/5 welding parameters. However, the minimum LSFL value was acquired from the joint of Case I using 3000/3/2.45/5 and from the joint of Case II 3000/3/2.45/10 welding parameters. Different weld geometries can be seen for both types of joints made at different welding parameters. In lap-shear tensile tests, mainly two different fracture morphologies were observed for both of Case I and Case II: the pull-out nugget and cross-nugget failure (Fig. 5) [24]. The joint which exhibited a low LSFL value failed with a cross-nugget failure mode as shown in Fig. 5a and c. Therefore, cross-nugget fracture occurs easily leading to a low LSFL value as discussed by [25]. On the other hand, pull-out nugget fracture mode was observed in the joint displaying maximum LSFL value as shown in Fig. 5b and d, which was also reported in several other works [15,16].

In the FSSW, on fracture mode is very important to check the excessive heat and pressure, because excessive heat and pressure can cause to fracture mode changes. Suitable welding parameters produce more heat and a big weld area which cause a high weld strength. In fact, a changes of the welding parameters result in more extensive stirring and higher heat input during FSSW, which develops the outdated thickness [26].

3.2. Signal-to-noise ratio

The signal-to-noise (S/N) ratio is a term that originated from the telecommunications field. It was applied in quality engineering by Genichi Taguchi. Some measurable responses to the system output during the operation of any engineering system or process are called performance characteristics [27]. The LSFL data were analyzed to determine the effect of FSSW process parameters. The experimental results were transformed into means and S/N ratio. The mean S/N ratio for welding parameters at levels 1, 2, and 3 can be calculated by averaging S/N ratios for the experiments 1–3, 4–6, and 7–9, respectively [28].

The LSFL is the main characteristic recognized to define the quality of FSSW joints of Case I and Case II sheets. In order to evaluate the influence of the welding parameters on the response, the means and S/N for each welding parameter were calculated. The S/N ratio of the LSFL was analyzed according to the principles of "the larger – the better" characteristic which can be explained as follows [22]. The S/N ratio is the ratio of the mean to the square deviation. Taguchi uses S/N ratio to measure the quality characteristic deviating from the desired value. The S/N ratio (η) is defined as [29].

$$\eta = -10\log(\mathrm{MSD}) \tag{1}$$

where MSD is the mean square deviation for the output characteristic.

$$\mathrm{MSD} = \frac{1}{n}\sum_{i=1}^{n}\frac{1}{T_i^2} \tag{2}$$

where n is the number of tests and T_i is the value of LSFL of the ith test. Tables 4 and 5 show the experimental results for the LSFL and the corresponding S/N ratio which were calculated by using Eqs. (1) and (2). These data were plotted for Case I and Case II as shown in Figs. 6 and 7. As shown in Tables 4 and 5, the lap-shear tensile test results exhibited that the FSSW of Case I and Case II conditions obtained the maximum LSFL 4.97 and 5.38 kN, respectively. The lowest LSFL is 2.64 and 4.64 kN for Case I and Case II conditions.

The graphs of Figs. 6 and 7 show the level effects of each welding parameter. It is clearly observed that the tool rotational speed has the biggest effect on the LSFL for Case I and II. Actually, these results are usually expected. The tool rotational speed is specially preferred for final FSSW. The total mean S/N ratio of the nine experiments was calculated as 11.55 dB for Case I as shown in Fig. 6 by a dashed line.

The S/N ratio was calculated as 14.13 dB for Case II as shown in Fig. 7 by a dashed line. For example, the mean S/N ratio increases from C1 to C3 for Case I and the mean S/N ratio decreases from B1 to B3 for Case II.

3.3. Analysis of variance

The analysis of variance (ANOVA) test was performed to identify the welding parameters that are statistically significant. The purpose of the ANOVA test is to investigate the significance of the welding parameters which affect the weld strength of FSSW joints. It gives a clear outlook as to how far the process parameter influences the response and the level of significance of the factor considered [30].

The percentage of the contribution of the tool rotational speed, tilt angle, tool plunge depth, and dwell time are shown for Case I

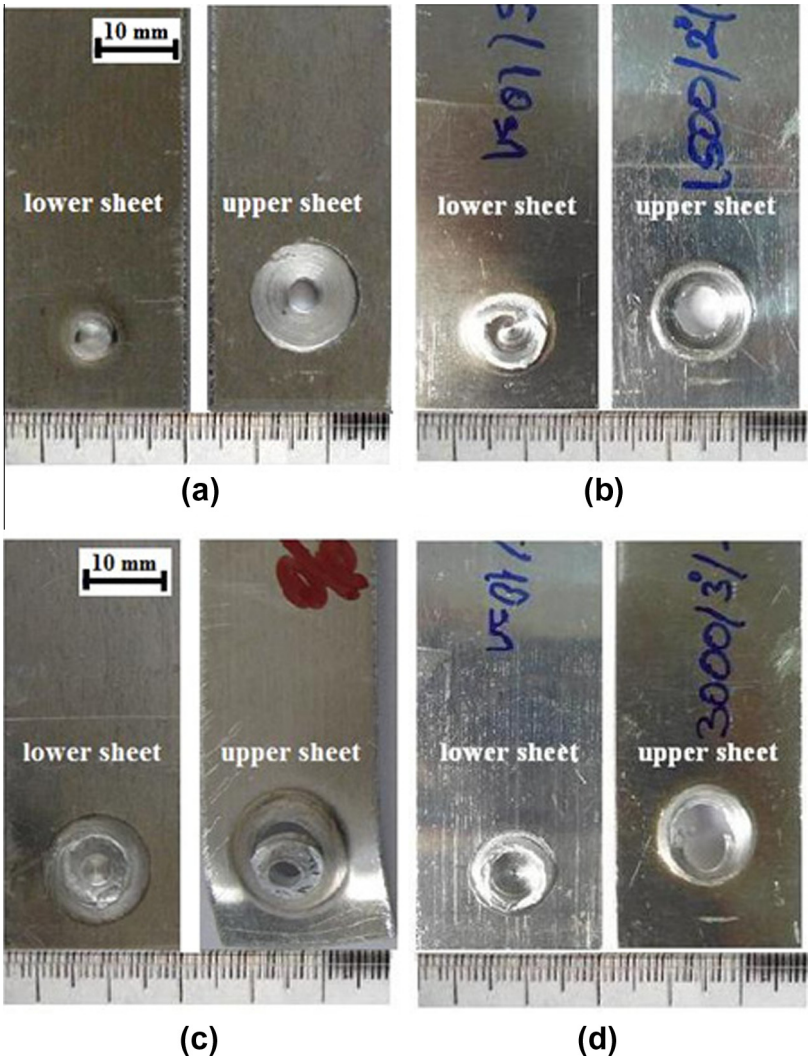


Fig. 5. Fracture surfaces of upper and lower sheets of dissimilar joints after lap-shear tensile tests: (a) and (b) FSSW joints of Case I and (c) and (d) FSSW joints of Case II.

Table 4
Experimental LSFL results and calculated S/N ratios for Case I.

Experiment number	LSFL (kN)	Calculated S/N ratio (dB)
1	4.50	13.06
2	4.97	13.93
3	4.77	13.57
4	3.71	11.39
5	4.23	12.53
6	2.64	8.43
7	3.53	10.96
8	3.57	11.05
9	2.86	9.13

Table 5
Experimental LSFL results and calculated S/N ratios for Case II.

Experiment number	LSFL (kN)	Calculated S/N ratio (dB)
1	5.18	14.29
2	5.38	14.62
3	5.10	14.15
4	5.30	14.49
5	5.35	14.57
6	5.17	14.27
7	4.92	13.84
8	4.64	13.33
9	4.83	13.68

and Case II in Tables 6 and 7. The percentage of the contribution is a function of the sum of squares for each significant item; it indicates the relative power of a factor to reduce the variation. If the factor levels are controlled precisely, then the total variation could be reduced by the amount indicated by the percentage of the contribution.

The high contribution value indicates that the factor is highly significant in affecting the response of the process. In this study, the tool rotational speed (factor A) and tilt angle (factor B) are a highly significant factor and play a major role in affecting the LSFL of the weld as shown in Fig. 6 and Table 6.

The effect of each control factor upon the welding parameters can be observed in Tables 6 and 7. The welding parameters can affect the arithmetic mean of absolute the LSFL which are given in Table 6. The most important factor in Case I on the LSFL is the tool rotational speed, which explains 53.66% contribution of

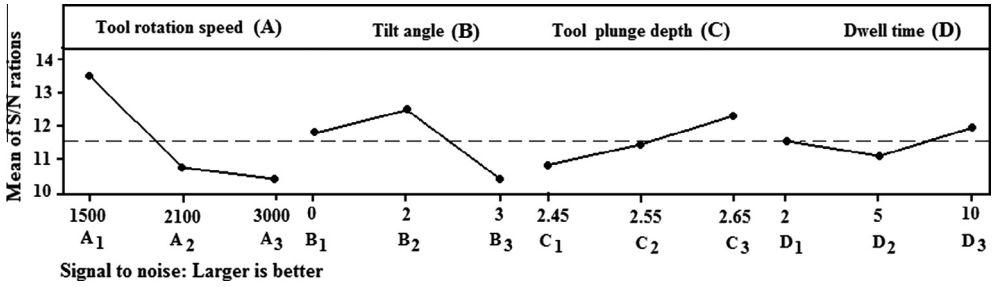


Fig. 6. The main effect plot for S/N ratio graph for Case I.

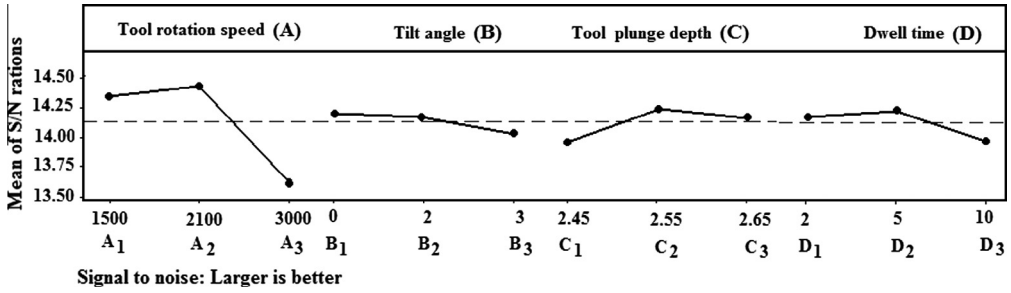


Fig. 7. The main effect plot for S/N ratio graph for Case II.

Table 6
Results of the ANOVA for LSFL of Case I.

Symbol	Welding parameters	Degrees freedom	Sum of squares	Mean square	*F* ratio	Contribution (%)
A	Tool rotation speed	2	12.9230	6.4615		53.66
B	Tilt angle	2	5.7180	2.8590		23.74
C	Tool plunge depth	2	3.0202	1.5101		12.54
D	Dwell time		1.3130	0.6565		5.45
Error		2	1.1125	0.6562		4.61
TOTAL		8	24.0867			100.0

Table 7
Results of the ANOVA for LSFL of Case II.

Symbol	Welding parameters	Degrees freedom	Sum of squares	Mean square	*F* ratio	Contribution (%)
A	Tool rotation speed	2	16.9331	8.4665		57.60
B	Tilt angle	2	3.0581	1.5290		10.40
C	Tool plunge depth	2	1.6501	0.8250		5.62
D	Dwell time		6.4422	3.2211		21.92
Error		2	1.3125	0.6562		4.46
Total		8	29.3960			100.0

the total variation. The next contribution on LSFL comes from the tilt angle (factor B) 23.74% and with the contribution tool plunge depth and with the contribution dwell time, 12.54% and 5.45%, respectively.

For Case II, the most important factor on the LSFL is the tool rotational speed, which explains 57.60% contribution of total variation as shown in Table 7. The next contribution on LSFL gives rise to the dwell time (factor D) 21.92% and with the contribution tilt angle and with the contribution tool plunge depth 10.40% and 5.60%, respectively.

3.4. Interpretation of experimental results

Both Case I and Case II tests, nine different welding parameter combinations were used. Therefore, the effect of each welding parameter on the LSFL cannot be clearly understood from the results of Tables 6 and 7. For his reason, a MINITAB 15 statistical software [31] was used to explain the welding parameter effect. Figs. 8 and 9 were drawn to display the welding parameters' effects on the LSFL from the results of Tables 6 and 7. These diagrams show the combined effects of any two parameters on the LSFL. In each graph, one welding parameter effect was omitted. Only two parameters can be decided a diagram. The tool rotation speed between 1500 rpm and 2250 rpm gives the optimum LSFL for the Case I (Fig. 8). The black zones of the diagrams show the LSFL over 4.5 kN in Fig. 8. Because other parameters must be selected according to the tool rotation speed, these six diagrams show to include in Fig. 8 give only rough results. A definite optimum welding parameter combination can be determined from this figure.

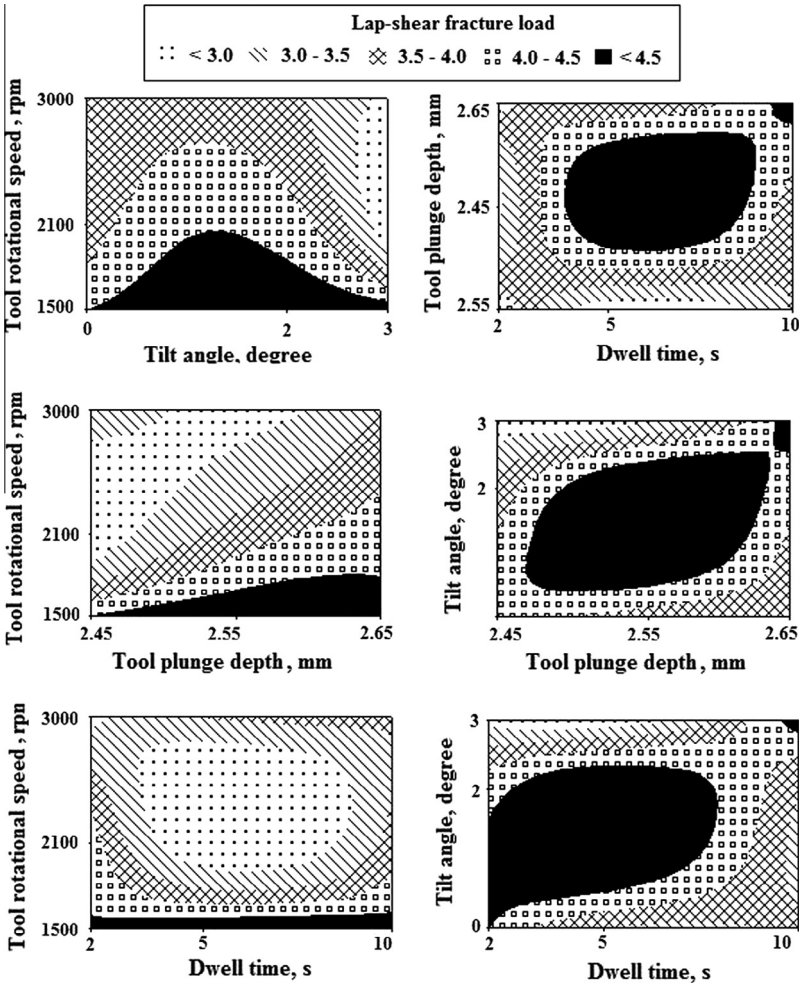


Fig. 8. ANOVA analyses the optimum welding parameters for LSFL of Case I.

For the Case II, the tool rotation speed between 1500 rpm and 2100 rpm gives the optimum LSFL (Fig. 9). The black zones of the diagrams show the LSFL over 5.3 kN. The most important factor on the LSFL is the tool rotational speed which explains 57.60% contribution of the total variation. Therefore, other welding parameters must be selected according to the tool rotation speed. For example in Case II, a definite optimum welding parameter combination can be determined from Fig. 9. The welding parameters such as tool rotational speed (1500–2100 rpm), tilt angle (0°–2.5°), tool plunge depth (2.48–2.65 mm), and dwell time (2–7 s) can be selected to obtain over 5.3 kN LSFL.

3.5. Confirmation test

The methods described in this work for LSFL prediction and optimization can eliminate the need for performing experiments. The purpose of this work is to identify the most effective welding parameter and percentage contribution of each parameter on LSFL of FSSW Case I and Case II joints. The final step is verifying the improvement in LSFL by conducting experiments using optimal conditions. The confirmation experiments were carried out by setting the process parameter at optimum levels. Once the optimal level of the design parameters has been determined, the final step is to predict and verify the improvement of the quality characteristic using the optimal level of the design parameters [32]. The predicted S/N ratio using the optimal welding parameters for LSFL is determined for Case I A1B2C3D3 and Case II A2B1C2D2 from S/N and ANOVA analysis. Five welds were performed with Case I using A1B2C3D3, and for Case II A2B1C2D2, welding parameters and their average LSFL were obtained. Tables 8 and 9 show the comparison of the predicted LSFL and experimental LSFL of these weld (Case I and Case II). The S/N ratio of the test was calculated for Case I and Case II by using Eqs. (1) and (2). There is a good agreement between the predicted and experimental LSFL values.

The initial parameters were chosen in Case I (A2B1C2D1) and Case II (A1B2C3D1) from Figs. 6 and 7. The experimental LSFL result and the calculated S/N ratio of the FSSW joint using Case I A1B2C3D3 and Case II A2B1C2D2 welding parameters are shown on the first column of Tables 8 and 9.

The welding parameters were set 1500/2/2.65/10 for Case I and 2100/0/2.55/5 for Case II. Five lap-shear tensile specimens were subjected to the average value of the FSSW joint. The tool rotational speed, tilt angle, tool plunge depth, and dwell time were set the average LSFL of FSSWed joint that was found to be for Case I (5.28 kN) and for Case II (5.64 kN), which were within the confidence interval of the predicted optimal of LSFL. The confirmation experiments show that the S/N ratio improved by 5.14 dB from the initial welding parameters to the optimal welding parameters and the LSFL is increased for Case I about 47%. But, there is no significant change in the LSFL of the Case II as 1.1%. It can be clearly seen that the better LSFL characteris-

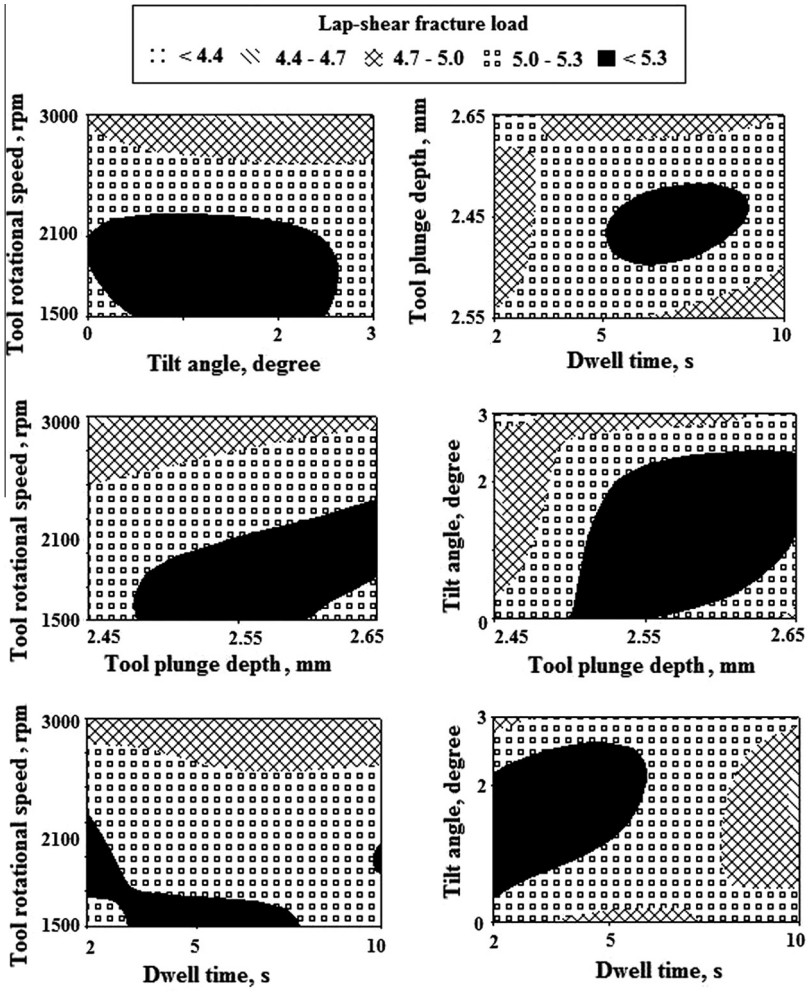


Fig. 9. ANOVA analyses the optimum welding parameters for LSFL of Case II.

Table 8
Results of the confirmation test for Case I.

	Initial welding (experiment)	Optimal welding parameters		Improvement
		Prediction	Experiment	
Parameter levels	A2B1C2D1	A1B2C3D3	A1B2C3D3	47%
LSFL (kN)	3.55	5.60	5.28	
Calculated S/N ratio (dB)	10.55	16.64	15.69	

Table 9
Results of the confirmation test for Case II.

	Initial welding (experiment)	Optimal welding parameters		Improvement
		Prediction	Experiment	
Parameter levels	A1B2C3D1	A2B1C2D2	A2B1C2D2	1.1%
LSFL (kN)	5.29	5.44	5.64	
Calculated S/N ratio (dB)	14.47	14.88	15.18	

tics are observed from the predicted welding parameters for Case I.

4. Conclusions

Based on the FSSW parameters, Case I and Case II sheets were studied by using the Taguchi method. The following results were obtained by the experimental and the analytic results:

(1) The L9 Taguchi orthogonal designed experiments of FSSW for Case I and Case II sheets were successfully conducted.
(2) The percentage of the contribution of FSSW parameters was evaluated. The highest growth was obtained from Case I joints. According to LSFL of joints for Case I, it was found that the tool rotational speed had 53.66%, tilt angle 23.74%, tool plunge depth 12.54%, and dwell time 5.45% contribution.

(3) The tool rotational speed played a vital role and contributed to both Case I and Case II, the overall response. The dwell time does not affect the response significantly in Case I. The tool plunge depth does not affect the response significantly in Case II
(4) In lap-shear tensile tests, mainly two different fracture morphologies were observed for both of Case I and Case II: the pull-out nugget maximum and cross-nugget failure minimum LSFL values.
(5) The improvement in the LSFL from the initial welding parameters to the optimal welding parameters was obtained for Case I about 47% from 3.55 to 5.28 kN and only 1.1% for Case II from 5.29 to 5.64 kN.

The positioning of the plates played an important role on the strength of the joints. The maximum LSFL value was acquired from the joint of Case I using 1500/2/2.65/10 welding parameters.

Acknowledgement

The authors are deeply grateful for the financial support of Marmara University Scientific Research Fund (BAPKO), Grant No. FEN-C-YLP-060911-0279.

References

[1] Yuan W, Mishra RS, Webb S, Chen YL, Carlson B, Herling DR, et al. Effect of tool design and process parameters on properties of Al alloy 6016 friction stir spot welds. J. Mater. Process. Technol 2011;211:972–7.
[2] Anawa EM, Olabi AG. Using taguchi method to optimize welding pool of dissimilar laser-welded components. Optics Laser Technol 2008;40:379–88.
[3] Fanelli P, Vivio F, Vullo V. Experimental and numerical characterization of friction stir spot welded joints. Eng Fract Mech 2012;81:17–25.
[4] Thomas WM, Nicholas ED, Needham JC, Murch MG, Temple-Smith P, Dawes CJ. International patent application no. PCT/GB92/02203 and GB patent application no. 9125978 and US patent application no. 5460317; December 1991.
[5] Mishra RS, Ma ZY. Friction stir welding and processing. Mater Sci Eng R 2005;R50(1–2):1–78.
[6] Nandan R, DebRoy T, Bhadeshia HKDH. Recent advances in friction stir welding process, weldment structure and properties. Prog Mater Sci 2008;53(6): 980–1023.
[7] Threadgill PL, Leonard AJ, Shercliff HR, Withers PJ. Friction stir welding of aluminium alloys. Int Mater Rev 2009;54(2):49–93.
[8] Çam G. Friction stir welded structural materials beyond Al-alloys. Int Mater Rev 2011;56(1):1–48.
[9] Tran VX, Pan J, Pan T. Effects of processing time on strengths and failure modes of dissimilar spot friction welds between aluminum 5754-O and 7075-T6 sheets. J Mat Proc Technol 2009;209:3724–39.
[10] Wang DA, Lee SC. Microstructures and failure mechanisms of friction stir spot welds of aluminum 6061-T6 sheets. J. Mater. Process. Technol 2007;186(1–3):291–7.
[11] Kulekci MK, Esme U, Er O. Experimental comparison of resistance spot welding and friction stir spot welding processes for the EN AW 5005 aluminum alloy. Mater Tehnol 2011;45(5):395–9.
[12] Bilici MK, Yukler AI, Kurtulmus M. The optimization of welding parameters for friction stir spot welding of high density polyethylene sheets. Mater Des 2011;32:4074–9.
[13] Eşme U. Application of taguchi method for the optimization of resistance spot welding process. Arab J Sci Eng 2009;34(2B):519–28.
[14] Mitlin D, Radmilovic V, Panc T, Chena J, Feng Z, Santella ML. Structure–properties relations in spot friction welded (also known as friction stir spot welded) 6111 aluminum. Mater Sci Eng A 2006;441:79–96.
[15] Buffa G, Fratini L, Piacentini M. On the influence of tool path in friction stir spot welding of aluminum alloys. J Mater Proc Technol 2008;208:309–17.
[16] Bozkurt Y, Salman S, Çam G. Investigation of friction stir spot welds of AA2024 and AA5754 Al-alloy sheets. In: 2nd Int Conf Weld Tech Exh 23–25 May, Ankara–Turkey; 2012. p. 357–368.
[17] Yamamoto M, Gerlich A, North TH, Shinozaki K. Cracking in the stir zones of Mg-alloy friction stir spot welds. J Mater Sci 2007;42:7657–66.
[18] Khan MI, Kuntz ML, Su P, Gerlich A, North T, Zhou Y. Resistance and friction stir spot welding of DP600: a comparative study. Sci Technol Weld Join 2007;12(2):175–82.
[19] Gerlich A, Su P, North TH, Bendzsak GJ. Friction stir spot welding of aluminum and magnesium alloys. Mater Forum 2005;29:290–4.
[20] Miyagawa K, Tsubaki M, Yasui T, Fukumoto M. Spot welding between aluminium alloy and low-carbon steel by friction stirring. Weld Int 2009;23(8):559–64.
[21] Chen YC, Nakata K. Effect of tool geometry on microstructure and mechanical properties of friction stir lap welded magnesium alloy and steel. Mater Des 2009;30:3913–9.
[22] Bozkurt Y. The optimization of friction stir welding process parameters to achieve maximum tensile strength in polyethylene sheets. Mater Des 2012;35:440–5.
[23] Specimens dimensions and procedure for shear testing resistance spot and embossed projection welded joints. JIS Z 3136, Japanese Standards Association, Tokyo, Japan; 1999.
[24] Fratini L, Barcellona A, Buffa G, Palmeri D. Friction stir spot welding of AA6082-T6: influence of the most relevant process parameters and comparison with classic mechanical fastening techniques. J Eng Manuf 2007;221:1111–8.
[25] Tozaki Y, Uematsu Y, Tokaji K. Effect of processing parameters on static strength of dissimilar friction stir spot welds between different aluminium alloys. Fat Fract Eng Mater Struct 2007;30:143–8.
[26] Pouranvari M, Asgari HR, Mosavizadch SM, Marashi PH, Goodarzi M. Effect of weld nugget size on overload failure mode of resistance spot welds. Sci Technol Weld Join 2007;12:217–25.
[27] Shiang SJ, Fong TY, Bin YJ. Principal component analysis for multiple quality characteristics optimization of metal inert gas welding aluminum foam plate. Mater Des 2011;32:1253–61.
[28] Lin TR. Experimental design and performance analysis of TiN coated carbide tool in face milling stainless steel. J Mater Proc Techn 2002;127:1–7.
[29] Peace GS. Taguchi methods. New York: Addison-Wesley; 1993.
[30] Vijayan S, Raju R, Subbaiah K, Sridhar N, Rao SRK. Friction Stir Welding of Al–Mg Alloy optimization of Process Parameters using taguchi method. Exp Technol 2010:37–44.
[31] Minitab User Manual (Release 15). Making data analysis easier. PA (USA): MINITAB Inc. State College; 2001.
[32] Mazundar SK, Hoa SV. Application of taguchi method for process enhancement of on-line consolidation technique. Composites 1995;26:669–763.